STRUCTURE AND CHARACTERISTICS OF Er^{3+} DOPED ZrO_2/CuO FOR PHOTOCATALYTIC DEGRADATION OF METHYLENE BLUE UNDER VISIBLE LIGHT

Pham Van Huan
Electric Power University

ARTICLE INFO

Received: 03/6/2024
Revised: 10/7/2024
Published: 11/7/2024

KEYWORDS

Nano ZrO_2/CuO:Er^{3+}
Photocatalysis
Co-precipitation
Methylene blue
Nanocomposite

ABSTRACT

Wastewater pollution containing organic pigments that are difficult to decompose is a global problem, and the photocatalytic method is currently a superior method. However, current photocatalytic materials are mainly active when illuminated by UV radiation. In this study, Er^{3+}-doped ZrO_2/CuO nanocomposite materials were synthesized by co-precipitation method, with photocatalytic activity under visible light. Characteristics of ZrO_2/CuO:Er^{3+} were investigated by scanning electron microscope (SEM), Energy-dispersive X-ray spectroscopy (EDS), transmission electron microscope (TEM), X-ray diffraction (XRD), diffuse reflectance spectrum (DRS). The obtained ZrO_2/CuO:Er^{3+} nanocomposite particles have an average diameter of about 12 - 14 nm. XRD shows that ZrO_2 forms tetragonal phase, CuO forms monoclinic phase. The photocatalytic properties of the material under simulated sunlight degradation 95% of methylene blue (20 mg.L^{-1}) in 210 minutes with a degradation constant of $k_{app} = 6.87\times10^{-3}$ min^{-1}. Research shows that Er^{3+}-doped ZrO_2/CuO nano composite materials have potential applications in the field of textile wastewater treatment and wastewater pollution treatment with sunlight.

CẤU TRÚC VÀ ĐẶC TRƯNG TÍNH CHẤT CỦA ZrO_2/CuO PHA TẠP Er^{3+} CHO XÚC TÁC QUANG PHÂN HỦY XANH METYLEN DƯỚI ÁNH SÁNG KHẢ KIẾN

Phạm Văn Huấn
Trường Đại học Điện lực

THÔNG TIN BÀI BÁO

Ngày nhận bài: 03/6/2024
Ngày hoàn thiện: 10/7/2024
Ngày đăng: 11/7/2024

TỪ KHÓA

Nano ZrO_2/CuO:Er^{3+}
Quang xúc tác
Đồng kết tủa
Xanh Methylene
Nanocomposite

TÓM TẮT

Ô nhiễm nước thải có chứa chất màu hữu cơ khó phân hủy là một vấn đề toàn cầu, phương pháp quang xúc tác đang là phương pháp nhiều ưu việt. Tuy nhiên các vật liệu quang xúc tác hiện nay chủ yếu có hoạt tính khi được chiếu sáng bởi bức xạ UV. Trong nghiên cứu này vật liệu nano composite ZrO_2/CuO pha tạp Er^{3+} được tổng hợp bằng phương pháp đồng kết tủa, có hoạt tính quang xúc tác dưới ánh sáng khả kiến. Đặc tính của ZrO_2/CuO:Er^{3+} được khảo sát bằng kính hiển vi (SEM), phổ tán sắc năng lượng tia X (EDS), (TEM), XRD, phổ phản xạ khuếch tán (DRS). Các hạt nanocomposite ZrO_2/CuO:Er^{3+} thu được có đường kính trung bình khoảng 12 - 14 nm. XRD cho thấy ZrO_2 hình thành pha tetragonal, CuO hình thành pha monoclinic. Tính chất quang xúc tác của vật liệu dưới ánh sáng mặt trời mô phỏng phân hủy 95% MB (20 mg.L^{-1}) trong thời gian 210 phút với hằng số phân hủy là $k_{app} = 6.87\times10^{-3}$ min^{-1}. Nghiên cứu cho thấy vật liệu nano composite ZrO_2/CuO pha tạp Er^{3+} có tiềm năng ứng dụng trong lĩnh vực xử lý nước thải dệt nhuộm, xử lý ô nhiễm nước thải dưới ánh sáng mặt trời.

DOI: https://doi.org/10.34238/tnu-jst.10519

Email: phamhuannb@gmail.com

1. Introduction

Water pollution caused by industrial wastewater containing toxic organic substances is increasingly serious. One of the approaches to treat wastewater pollution is to use photocatalysis. This method has many advantages such as not creating secondary pollutants, using sunlight energy directly, being environmentally friendly and cheap. Photocatalysis uses semiconductors that absorb photon energy from radiation to accelerate the photoreaction [1]. Photocatalysts fall into three main groups: Heterogeneous, homogeneous and plasmonic reaction catalysts. A series of semiconductor oxides such as TiO_2, ZnO, CeO_2 and ZrO_2 have been used as photocatalysts and studied and reported [2] - [4]. However, the application of the above semiconductor oxides is greatly limited, due to high electron-hole pair recombination, and the material only absorbs light in the ultraviolet region.

Zirconia (ZrO_2) is an important known multipurpose material and an extremely versatile semiconductor with applications in photocatalysis, biosensing, it is famous for its high mechanical strength, inertness Chemically, good biocompatibility, often used in dental implants or coatings on orthopedic implant materials [5], [6] ZrO_2 has a wide band gap E_g and a negative value high of the conduction potential, its band gap ranges from 3.25 eV to 5.10 eV, depending on the preparation method [7]. Due to the large band gap, the oxidation potentials of ZrO_2 are very high, which is essential for semiconductors used in photocatalysis. However, the photocatalytic activity of ZrO_2 can only be activated by short-wavelength light, which accounts for about 4% of solar energy, which is a major barrier for its practical application. To improve the photocatalytic ability of ZrO_2 in the visible light region, many methods have been proposed such as: doping, co-doping with metal or non-metal ions, combining with light-sensitive dyes, or combining compatible with other semiconductor oxides [8], [9]. Many previous studies have shown that ZrO_2 when combined with other semiconductor oxides has the ability to enhance photocatalysis, due to efficient charge separation and effective charge transfer between electrons. and holes from one semiconductor to another [10], [11]. Semiconducting oxides, when introduced with ZrO_2, act as a light sensitizer, by shifting the absorption wavelength from the ultraviolet region to the visible region, due to the change in the band gap of the composite material. This leads to the charge transfer of electrons and holes occurring easily. The recombination of electron and hole pairs is inhibited, so photocatalytic activity is enhanced.

Among miscible metal oxides, CuO is a suitable semiconductor oxide, because CuO has photocatalytic activity at room temperature, low cost and narrow energy gap (1.90 eV) [12]. However, photocatalysts with a narrow energy gap can be activated by visible light, but they have a low oxidation potential and cannot oxidize organic compounds with a stable ring structure [13]. For example, phenyl compounds are almost not completely oxidized by visible light photocatalytic reactions. Therefore, it is necessary to develop hierarchical structures between CuO and other semiconductor oxides. Wang, Xiao-Ning and co-workers reported, CuO/ZrO_2 catalyst is a stable catalyst for H_2 formation from oxalic acid solution, under simulated sunlight [14]. Yan Jian-hui and co-workers reported, synthesizing CuO/ZrO_2 by solid and co-precipitation method, to evaluate photocatalytic hydrogen splitting, under simulated sunlight irradiation [15].

The use of sunlight over a wide range, from the ultraviolet (UV) to the near infrared (NIR), is becoming an attractive topic in the field of photocatalysis. One of the options is based on the incorporation of a rare earth ion into the structure of the photocatalytic material [16]. Doping with rare earth ions has been proven to be an effective method, to improve photocatalytic properties, because of the rare earth ions with 4f shell and empty 5d orbitals, the incorporation of rare earth ions into the host lattice can inhibit the recombination of electron and hole pairs. Among rare earth ions, Er^{3+} possesses the most abundant energy level structure in the IR-UV range, Er^{3+} has the ability to emit upconversion according to the appropriate excitation wavelength. They can emit high-intensity radiation in the UV, visible and near-infrared (NIR)

regions, allowing photocatalytic activation of semiconductors with narrow to wide bandgap [17], [18]. Through photocatalysis occurs under visible light, and even near infrared [19].

In this study, ZrO_2/CuO doped with Er^{3+} was synthesized by co-precipitation method, which is simple and highly economical. The ZrO_2 /CuO catalyst can increase the decomposition efficiency of methylene blue (MB), and Er^{3+} doping can enhance the absorption extension to the infrared region. The effect of Er^{3+} doping on photocatalytic properties has been systematically studied. The grain size, crystal phase, band gap and upconversion fluorescence of Er^{3+}-doped ZrO_2/CuO were also investigated.

2. Materials and Methods

Chemicals: $ZrOCl_2.8H_2O$ (99.9%, Aldrich, Saint Louis, USA), $CuCl_2.2H_2O$ (99.9%, Aldrich, Saint Louis, USA), and $ErCl_3.6H_2O$, Cetyl trimethyl ammonium bromide (CTAB - 99.9%, Merck). NH_3 concentration 30% (99.9%, Merck, Germany), Methylene blue (99%), were purchased from Xilong Scientfic.

Synthesis of ZrO_2/CuO:Er^{3+}: In a typical experiment, 5 mmol $ZrOCl_2.8H_2O$ and 2.5 mmol $CuCl_2.2H_2O$ and 20 mg CTAB (as a surfactant) are dissolved in 100 mL^{-1} distilled water for 30 minutes. Er^{3+} ions were added at an appropriate mol% doping ratio from the $ErCl_3$ salt solution. Precipitate the solution by adding a sufficient amount of NH_3 solution and stirring on a magnetic stirrer for 2 hours. The solution was centrifuged to obtain the precipitate, and the precipitate was washed with distilled water and ethanol solution. ZrO_2/CuO:Er^{3+} powder was dried at 80 °C for 2 hours for further studies.

Photocatalytic properties of ZrO_2 /CuO:Er^{3+} : 10 mg of ZrO_2/CuO:Er^{3+} was added to 25 mL of methylene blue solution (20 $mg.L^{-1}$), the solution was stir continuously in the dark for 1 hour to equilibrate the MB adsorption. A xenon lamp (power 100 W) was used as the visible light source. After each period of 30 minutes the sample will be taken out, and the solution will be tested for the remaining MB concentration using UV-Vis spectroscopy. The degredation efficiency of MB is calculated according to formula (1).

$$H = \frac{C_0 - C}{C_0} \times 100 \quad (1)$$

In which: C_0 is the initial methylene blue concentration ($mg.L^{-1}$), C is the methylene blue concentration after each lighting period.

ZrO_2/CuO:Er^{3+} nanoparticles were characterized by X-ray diffraction (XRD, D8 Advance, Bruker). The microstructure of ZrO_2/CuO:Er^{3+} nanoparticles was analyzed using a scanning electron microscope (JEOL, JEM 1010, JEOL Techniques, Japan, located at Hanoi University of Science and Technology). To investigate the chemical bond of the material, infrared (IR) absorption spectra were recorded in the wavenumber range from 4000 cm^{-1} to 400 cm^{-1} with a Perkin-Elmer Spectrum BX spectrometer using KBr pellets. Diffuse reflectance spectra were measured on a Cary 5000 from Agilent, USA.

3. Results and Discussion

3.1. Phase formation of ZrO_2 /CuO:Er^{3+}

Figure 1 (a) shows the X-ray diffraction pattern of ZrO_2/CuO:Er^{3+} nanoparticles synthesized by co-precipitation method. XRD shows that the obtained material has good crystallinity as shown by sharp diffraction peaks. Including tetragonal crystal phase of ZrO_2 and monoclinic crystal phase of CuO.

The diffraction peaks were observed at angles 2 theta = ~ 30.2°, 35.4°, 50.3° and 60.2°, corresponding to the lattice planes (011), (200), (112) and (121) is the structure of the tetragonal phase of ZrO_2 crystal (according to standard card JCPDS 50-1089) [20]. ZrO_2 crystals have three forms existing in three different phases or simultaneously tetragonal, cubic and monoclinic

phases depending on the synthesis method. In the co-precipitation method using CTAB, ZrO_2 forms in the tetragonal phase.

The diffraction peak positions of CuO are shown at angle 2 theta = ~ 35.5° (002), 38.8° (111), 48.5°(-202), 53.8°(020), 58.2°(202), 61.5°(-113), 66.0° (022), and 68.1° (220). Corresponding to the crystal face of CuO belonging to the monoclinic phase (according to standard card JCPDS 48-1548). No peaks for Er_2O_3 or foreign doping were observed at all Er^{3+} doping concentrations.

This may be because Er^{3+} has replaced Zr^{4+} in the host matrix. On the other hand, when the Er^{3+} doping concentration increases, the diffraction peak (100) of the tetragonal ZrO_2 phase tends to shift toward the smaller 2 theta angle than shown in Figure 1 (b). This can be explained as the Er^{3+} ion (1.20 Å) has a larger ionic radius than the Zr^{4+} (1.03 Å), which when doped causes the crystal lattice to expand [21].

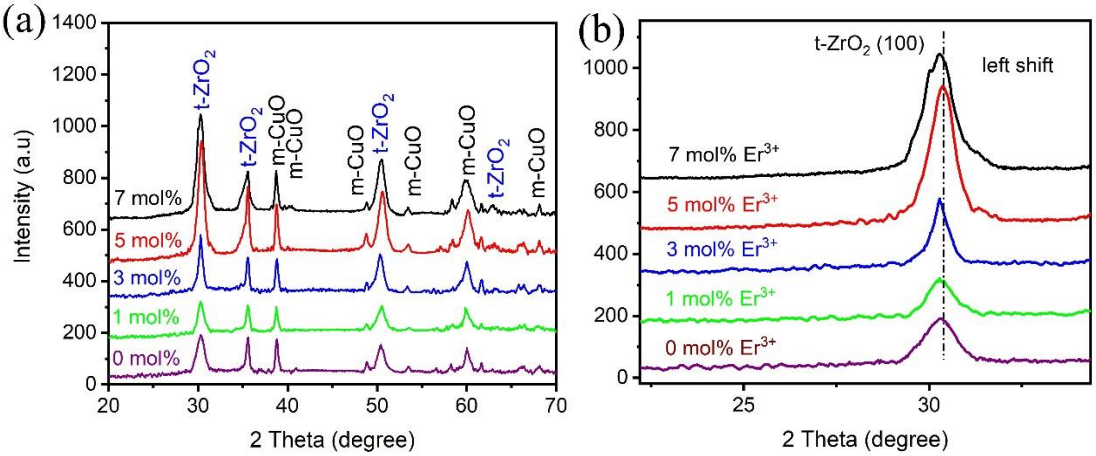

Figure 1. *(a) XRD powder diffraction pattern and (b) zoom at 2 theta = ~ 30.2° of ZrO_2/CuO and Er^{3+} doped ZrO_2/CuO*

3.2. Optical properties of ZrO_2/CuO:Er^{3+}

Figure 2 (a) show that ZrO_2/CuO nanocomposite have a strong absorption peak at 220 nm and a peak at 290 nm. These peaks in the UV region are believed to originate from charge transfer from O^{2-} to Zr^{4+} [22]. When doping increasing concentrations of Er^{3+} ions into the crystal lattice of ZrO_2/CuO nanocomposite, it shows that the absorption region extends to the visible region of 600 - 800 nm. This is attributed to the d - d transition band of the octahedral coordinated Cu^{2+} ion, which shifts the absorption band in the visible region in ZrO_2 /CuO. To calculate the band gap of semiconductors, people often use the Tauc relation described by the following equation [23].

$$\alpha h\nu = A(h\nu - E_g)^n \quad (2)$$

α, h, ν is absorption coefficient, Planck's constant, the frequency of incident photon, respectively, E_g is the optical band gap, A is a constant that depends on the transition probability. And n is an index that depends on the nature of the semiconductor. For direct junction semiconductors, the value is n = 1/2 and for indirect junction semiconductors, n = 2.

Figure 2 (b) shows that the band gap of ZrO_2 /CuO is found to be 3.38 eV. Increasing the Er^{3+} doping ratio leads to a decrease in the band gap and a red shift down to 2.68 eV. The decrease in the band gap of ZrO_2/CuO when doped with Er^{3+} is due to the appearance of the Er^{3+} impurity band formed by overlapping impurity states. It can be said that the band gap is reduced due to the synergistic effect of ZrO_2, CuO and Er^{3+} ions doped into the host matrix. The E_g values of the ZrO_2/CuO:x%Er^{3+} (x = 0 - 7) samples, decrease in the order of approximately 3.38, 3.17, 3.08, 3.00 and 2.68 eV, respectively.

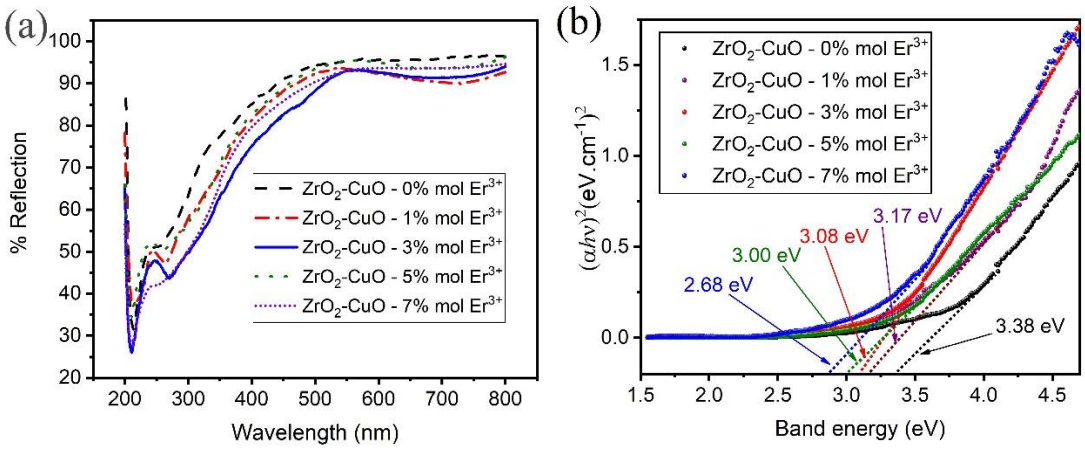

Figure 2. *(a) UV-Vis DRS spectra, (b)Tauc's plot*

3.3. Morphology of the material

Figure 3 (a) shows SEM images of Er^{3+} doped ZrO_2/CuO with concentrations 5 mol% Er^{3+}. The Er^{3+} doped ZrO_2/CuO is nearly spherical particles with nanometer size, the diameter of the particles is about 6 nm - 20 nm.

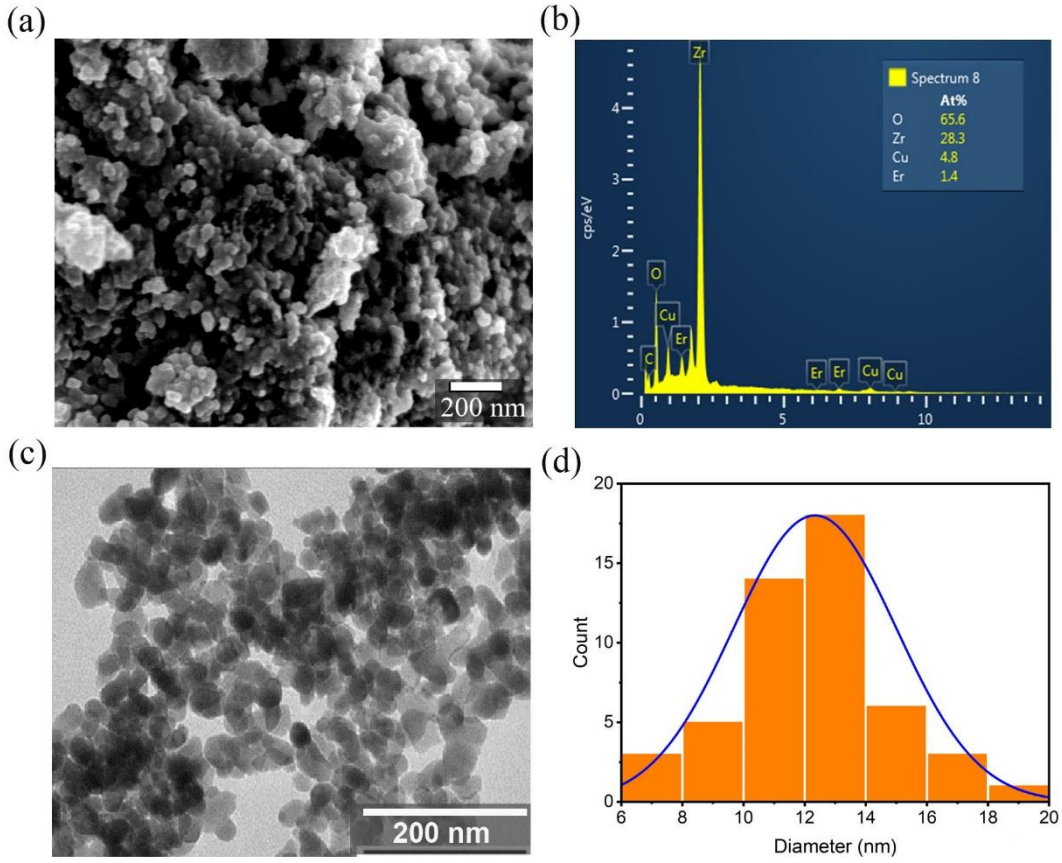

Figure 3. *(a) SEM image, (b) EDS spectrum, (c) TEM image and (d) particle size distribution of ZrO_2/CuO doping with 5 mol% Er^{3+}*

Figure 3 (b) show the high energy scattering spectrum (EDS) of ZrO_2/CuO doped with Er^{3+} ions, the results confirmed the presence of Zr elements, Cu, O and Er. Combined with the above

XRD analysis results, it is confirmed that ZrO_2/CuO nanocomposite particles doped with Er^{3+} ions have effectively doped into the matrix.

The TEM images shown in Figure 3(c) and Figure 3(d) are particle size distribution graphs according to the diameter of the particles (ImageJ image analysis software was used for analysis). The results show that ZrO_2/CuO nanocomposite particles have particle diameters distributed from 6 nm - 20 nm. Particles with a diameter of 12 - 14 nm appear most frequently. Particles tend to agglomerate with each other, due to the surface effect of nano-sized particles. Small sized nanoparticles will have a large specific surface area and will easily adsorb organic substances to the surface, which will be favorable conditions for photocatalytic reactions to occur.

3.4. Photocatalytic properties of ZrO_2/CuO:Er^{3+}

Figure 4(a) shows absorbance of the MB solution continuously decreased after the illumination time, the degredation concentration of MB was calculated from the absorbance (at wavelength 665 nm). After 210 minutes of illumination, the concentration of MB solution decreased by up to 95%.

Figure 4(b) show that the MB degradation efficiency under visible light of ZrO_2 alone is not high, only reaching 17% after 210 minutes of illumination. For ZrO_2/CuO nanocomposite particles, the photocatalytic efficiency of MB degradation increases significantly compared to ZrO_2. Furthermore, doping Er^{3+} to ZrO_2/CuO increases the photocatalytic efficiency. The degradation efficiency of ZrO_2 /CuO doped with Er^{3+} at a concentration of 7 mol% is about 15% higher than that of ZrO_2/CuO. This can be explained by the fact that increasing Er^{3+} ion concentration reduces electron-hole recombination, leading to increased photocatalytic efficiency, similar to Ce^{3+}/Ce^{4+} ion doping in the lattice ZrO_2 /CuO matrix [24].

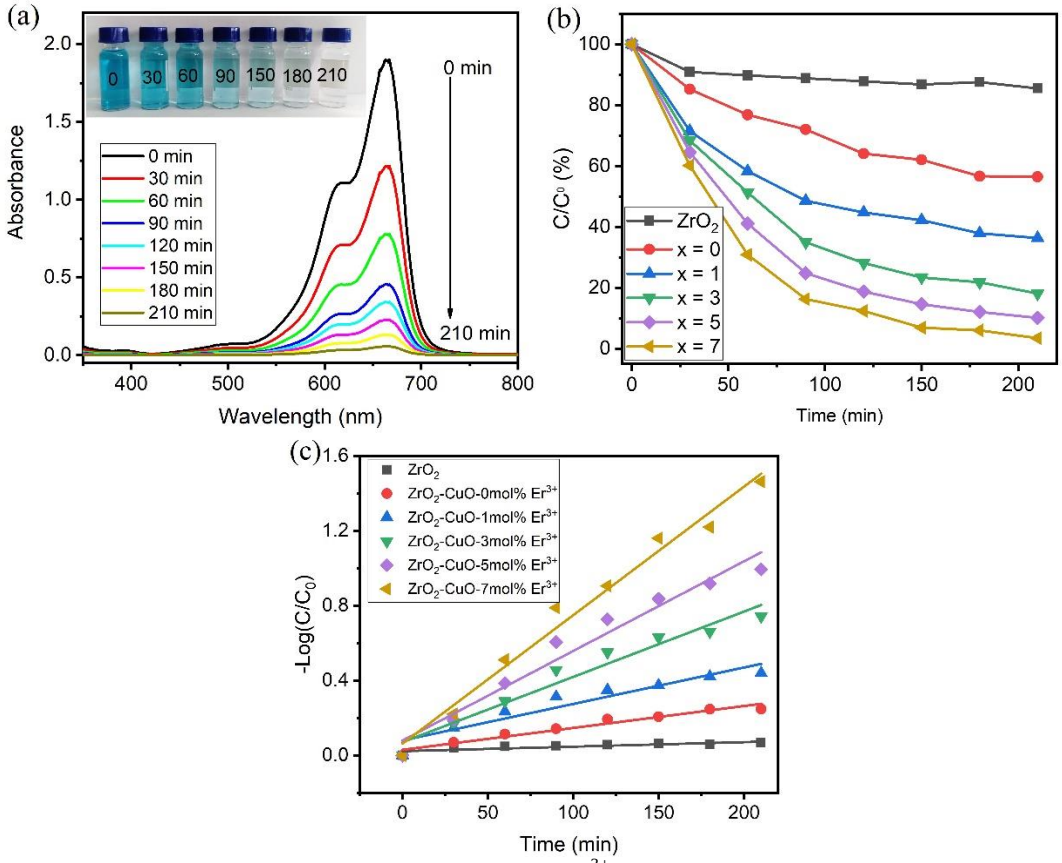

Figure 4. *(a) UV – Vis, (b) C/C_0 with differents Er^{3+} concentration doped, (c) linear fitting*

MB is degraded according to the first-order kinetic equation, the photocatalytic reaction rate constant k_{app} is determined by linearly fitting the graph of the relationship between $\ln(C/C_0)$ and t is the irradiation time radiation, k_{app} is calculated from the slope of the graph. Figure 4 (c) shows that the k_{app} value increases as the Er^{3+} doping concentration increases from 0 to 7 mol%. ZrO_2 has a very small value of $k_{app} = 2.9\times10^{-4}min^{-1}$; ZrO_2 /CuO the value of the constant is $k_{app} = 1.17\times10^{-3}$ min^{-1}; 1 mol% with $k_{app} = 1.95\times10^{-3}min^{-1}$; 3 mol% with $k_{app} = 3.49\times10^{-3}$ min^{-1}; 5 mol% with k_{app} $= 4.79\times10^{-3}$ min^{-1} and 7 mol% with $k_{app} = 6.87\times10^{-3}$ min^{-1}. It has been shown that ZrO_2/CuO doped with 7 mol% Er^{3+} has the highest $k_{app,}$ much higher than ZrO_2 and ZrO_2/CuO undoped with Er^{3+}. On the other hand, doping with Er^{3+} makes charge and hole separation in semiconductors more effective, reducing recombination, thereby effectively improving the photocatalytic activity of the material.

4. Conclusion

Er^{3+}-doped ZrO_2/CuO nanocomposite were synthesized by co-precipitation method, the resulting ZrO_2/CuO nanoparticles have an average diameter in the range of 12 - 14 nm. The Er^{3+} doped ZrO_2/CuO has photocatalytic activity under visible light. Methylene blue solution (20 $mg.L^{-1}$) degraded up to 95% when exposed to simulated sunlight radiation after 210 minutes. The superior photocatalytic performance of ZrO_2/CuO photocatalyst compared to ZrO_2 is explained by the effective charge transfer between CuO and ZrO_2, Er^{3+} doped ZrO_2/CuO prevents recombination of pair of electrons and holes. The Er^{3+}doped ZrO_2/CuO heterojunction nanocomposite system can extend the light harvesting range but also prolong and promote the lifetime and effective carrier separation, leading to high photocatalytic performance and can use visible light. The research has potential applications in the fields of textile wastewater pollution treatment in the water environment.

REFERENCES

[1] S. E. Braslavsky, “Glossary of terms used in photochemistry, 3rd edition (IUPAC Recommendations 2006),” *Pure Appl. Chem.*, vol. 79, no. 3, pp. 293–465, 2007.

[2] K. L. Chow *et al.*, "Removal of decabromodiphenyl ether (BDE-209) using a combined system involving TiO_2 photocatalysis and wetland plants," *Journal of hazardous materials*, vol. 322, pp. 263-269, 2017.

[3] A. D. Mauro *et al.*, "ZnO for application in photocatalysis: From thin films to nanostructures," *Materials Science in Semiconductor Processing*, vol. 69, pp. 44-51, 2017.

[4] S. R. Teeparthi, E. W. Awin, and R. Kumar, "Dominating role of crystal structure over defect chemistry in black and white zirconia on visible light photocatalytic activity," *Scientific reports*, vol. 8, no. 1, 2018, Art. no. 5541.

[5] R. Wang *et al.*, "Antimicrobial property, cytocompatibility and corrosion resistance of Zn-doped ZrO_2/TiO_2 coatings on Ti_6Al_4V implants," *Materials Science and Engineering: C*, vol. 75, pp. 7-15, 2017.

[6] T. Linkevicius, "The Novel Design of Zirconium Oxide-Based Screw-Retained Restorations, Maximizing Exposure of Zirconia to Soft Peri-implant Tissues: Clinical Report After 3 Years of Follow-up," *International Journal of Periodontics & Restorative Dentistry*, vol. 37, no. 1, pp.41-48, 2017.

[7] K. Kaviyarasu *et al.*, "Photocatalytic activity of ZrO_2 doped lead dioxide nanocomposites: Investigation of structural and optical microscopy of RhB organic dye," *Applied Surface Science*, vol. 421, pp. 234-239, 2017.

[8] E. S. Agorku, A. T. Kuvarega, B. B. Mamba, A. C. Pandey, and A. K. Mishra, "Enhanced visible-light photocatalytic activity of multi-elements-doped ZrO_2 for degradation of indigo carmine," *Journal of Rare Earths*, vol. 33, no. 5, pp. 498-506, 2015.

[9] B. Nanda, A. C. Pradhan, and K. M. Parida, "Fabrication of mesoporous CuO/ZrO_2-MCM-41 nanocomposites for photocatalytic reduction of Cr (VI)," *Chemical Engineering Journal*, vol. 316, pp. 1122-1135, 2017.

[10] B. M. Alajmi *et al.,* "Hierarchical mesoporous CuO/ZrO_2 nanocomposite photocatalyst for highly stable photoinduced desulfurization of thiophene," *Surfaces and Interfaces,* vol. 39, 2023, Art. no. 102899.

[11] X. Chen *et al.,* "Popcorn balls-like $ZnFe_2O_4$-ZrO_2 microsphere for photocatalytic degradation of 2, 4-dinitrophenol," *Applied Surface Science,* vol. 407, pp. 470-47, 2017.

[12] L. Xu *et al.,* "Investigation of optical bandgap variation and photoluminescence behavior in nanocrystalline CuO thin films," *Optik-International Journal for Light and Electron Optics,* vol. 158, pp. 382-390, 2018.

[13] N. Yahya *et al.,* "A review of integrated photocatalyst adsorbents for wastewater treatment," *Journal of Environmental Chemical Engineering,* vol. 6, pp. 7411-7425, 2018.

[14] X. –N. Wang *et al.,* "Two Self-Interpenetrating Copper (II)-Paddlewheel Metal–Organic Frameworks Constructed from Bifunctional Triazolate–Carboxylate Linkers," *Crystal Growth & Design,* vol. 18, no. 10, pp. 6204-6210, 2018.

[15] L. Renuka *et al.,* "A simple combustion method for the synthesis of multi-functional ZrO_2/CuO nanocomposites: Excellent performance as Sunlight photocatalysts and enhanced latent fingerprint detection," *Applied Catalysis B: Environmental,* vol. 210, pp. 97-115, 2017.

[16] L. Zhang, W. Z. Wang, S. M. Sun, Z. J. Zhang, J. H. Xu, and J. Ren, "Photocatalytic activity of Er^{3+}, Yb^{3+} doped Bi_5O_7I," *Catalysis Communications,* vol. 26, pp. 88–92, 2012.

[17] Y. Gao *et al.,* "Facile Synthesis of GdF_3: Yb^{3+}, Er^{3+}, Tm^{3+}@ TiO_2–Ag Core–Shell Ellipsoids Photocatalysts for Photodegradation of Methyl Orange Under UV, Visible, and NIR Light Irradiation," *Journal of Nanoscience and Nanotechnology,* vol. 18, no. 12, pp. 8216-8224, 2018.

[18] S. K. Ray *et al.,* "Photocatalytic degradation of Rhodamine B and Ibuprofen with upconversion luminescence in Ag-$BaMoO_4$: Er^{3+}/Yb^{3+}/K^+ microcrystals," *Journal of Photochemistry and Photobiology A: Chemistry,* vol. 339, pp. 36-48, 2017.

[19] Q. Ji *et al.,* "Photocatalytic degradation of diesel pollutants in seawater by using ZrO_2 (Er^{3+})/TiO_2 under visible light," *Journal of Environmental Chemical Engineering,* vol. 5, no. 2, pp. 1423-1428, 2017.

[20] S. Bhaskar *et al.,* "Design of nanoscaled heterojunctions in precursor-derived t-ZrO_2/SiOC (N) nanocomposites: Transgressing the boundaries of catalytic activity from UV to visible light," *Scientific Reports,* vol. 10, no.1, 2020, Art. no. 430.

[21] R. D. Shannon, "Revised effective ionic radii and systematic studies of interatomic distances in halides and chalcogenides," *Acta crystallographica section A: crystal physics, diffraction, theoretical and general crystallography,* vol. 32, no. 5, pp. 751-767, 1976.

[22] K. M. Parida and D. Rath, "Structural properties and catalytic oxidation of benzene to phenol over CuO-impregnated mesoporous silica," *Applied Catalysis A: General,* vol. 321, no. 2, pp. 101-108, 2007.

[23] J. Tauc, "Optical properties and electronic structure of amorphous Ge and Si," *Materials Research Bulletin,* vol. 1, pp. 37-46, 1968.

[24] M. N. Chu *et al.,* "Ce^{3+}/Ce^{4+}-Doped ZrO_2/CuO nanocomposite for enhanced photocatalytic degradation of methylene blue under visible light," *Toxics,* vol. 10, no.8, p.463, 2022.